Journal of Alloys and Compounds 853 (2021) 157386

Contents lists available at ScienceDirect

Journal of Alloys and Compounds

journal homepage: http://www.elsevier.com/locate/jalcom

Microwave dielectric properties of Li3Mg2NbO6-based ceramics with (MxW1-x)5+ (M = Li+, Mg2+, Al3+, Ti4+) substitutions at Nb5+ sites

Ping Zhang *, Manman Hao , Mi Xiao

School of Electrical and Information Engineering and Key Laboratory of Advanced Ceramics and Machining Technology of Ministry of Education, Tianjin University, Tianjin, 300072, PR China

ARTICLE INFO

Article history:
Received 29 July 2020
Received in revised form
18 September 2020
Accepted 27 September 2020
Available online 28 September 2020

Keywords:
$Li_3Mg_2Nb_{0.96}(M_xW_{1-x})_{0.04}O_6$
Microwave dielectric properties
Ion polarizability
W-based composite ions

ABSTRACT

$Li_3Mg_2Nb_{0.96}$ $(M_xW_{1-x})_{0.04}O_6$ (M = Li^+, Mg^{2+}, Al^{3+}, Ti^{4+}) ceramics were prepared by the solid-state reaction method. The sintering characteristics, microstructure, phase composition and microwave dielectric properties of $Li_3Mg_2NbO_6$ ceramics with equivalent substitution $((Li_{1/5}W_{4/5})^{5+}$, $(Mg_{1/4}W_{3/4})^{5+}$, $(Al_{1/3}W_{2/3})^{5+}$ and $(Ti_{1/2}W_{1/2})^{5+}$) at the Nb-site were investigated firstly. After sintering at 1150 °C for 4 h, all samples were single-phase of orthogonal structure. Due to the difference in ion polarizability of the substituted ions, the dielectric constant changed. The substitution of $(M_xW_{1-x})^{5+}$ in $Li_3Mg_2Nb_{0.96}$ $(M_xW_{1-x})_{0.04}O_6$ ceramics significantly reduced dielectric loss. The quality factor showed a similar trend with the average bond valence. Moreover, the study found that the substitution of W-based composite ions has a small effect on the τ_f values of $Li_3Mg_2NbO_6$ ceramics.

1. Introduction

In recent years, low-cost microwave dielectrics with high-quality factors have attracted considerable interest. Microwave dielectric materials should have low permittivity (ε_r), high-quality factor ($Q\times f$) and near-zero temperature coefficient of resonant frequency (τ_f) to reduce signal transmission delay and maintain signal quality [1–6]. However, many types of microwave dielectric ceramics with low $Q \times f$ values. Therefore, how to improve the properties of microwave dielectric ceramics is still the main research task [7–11].

Recently, lithium-based compounds [12–16] have received widespread attention due to their excellent properties, such as $Li_3Mg_2XO_6$ (X = Nb, Ta, Sb), Li_2O-MgO-BO_2 (B = Ti, Sn, Zr), $Li_2M_2A_3O_{12}$ (M = Zn, Ca; A = W, Mo) and $Li_4Ti_{5(1+x)}O_{12}$. The partial replacement of Mg^{2+} ions or Nb^{5+} ions of $Li_3Mg_2NbO_6$ ceramics by some cations (Ni^{2+}, Ca^{2+}, Mn^{2+}, Zn^{2+}, Co^{2+}, Sb^{5+}, Ta^{5+}, V^{5+}) greatly improved the properties of $Li_3Mg_2NbO_6$ ceramics [17–23]. Wu et al. [24] used the chemical bond theory to research the relationship between the lattice structure and properties of $Li_3Mg_2NbO_6$ ceramics. In addition, Wang and Zhang et al. [25–27] greatly improved the quality factor of $Li_3Mg_2NbO_6$ ceramics by replacing Nb^{5+} with Ti^{4+}, W^{6+} and Mo^{6+} ions. Zhou et al. [28] added a small amount of V_2O_5 and 0.6CuO-0.4B_2O_3 to $Li_2Ti_{0.75}(Mg_{1/3}Nb_{2/3})_{0.25}O_3$ ceramics, and effectively reduced the sintering temperature from 1170 °C to below 910 °C. The ultra-low loss and temperature stability properties of $LTMN_{0.25}$ + 2 wt% V_2O_5 and $LTMN_{0.25}$ + 1 wt% 0.6CuO-0.4B_2O_3 ceramics made them expected to be widely used in 5G mobile communication system. Previously, different sintering aids [29–32] such as Li_2O–B_2O_3–SiO_2, ZnO–B_2O_3–SiO_2, MgO–B_2O_3–SiO_2, B_2O_3 were added to reduce the sintering temperature of $Li_3Mg_2NbO_6$ ceramics. The research results showed that when 0.5 wt% ZBS was added, $Li_3Mg_2NbO_6$ ceramics achieved great dielectric properties when sintered at 925 °C for 4 h: ε_r = 14.3, $Q \times f$ = 73,987 GHz, τ_f = −16.05 ppm/°C.

Some scholars have replaced the B-site ions in lithium-based microwave dielectric ceramics with composite ions to enhance microwave dielectric properties. The microwave dielectric properties of $(Zn_{1/3}A_{2/3})_{0.5}(Ti_{1-x}B_x)_{0.5}O_2$ (A = Ta^{5+}, Nb^{5+}, B = Sn^{4+}, Ge^{4+}) ceramics [33] and $MgTi_{0.95}$ $(AB)_{0.05}O_3$ (A = Li^+, Mg^{2+}, Al^{3+}, B = Nb^{5+}, Ta^{5+}) ceramics [34] were investigated. Due to the decrease of Ti^{4+} ions, the $Q \times f$ values of the samples increased with the increase of BO_2 content [33]. The sintered samples with Ta^{5+} showed higher $Q \times f$ values and smaller ε_r than those with Nb^{5+} because of their higher average ionic bond valence [34]. In 2018, Wu et al. [35,36] used composite ions $(Mg_{1/3}Sb_{2/3})^{4+}$ and $(Mg_{1/3}Nb_{2/3})^{4+}$ to

* Corresponding author.
E-mail address: zptai@163.com (P. Zhang).

https://doi.org/10.1016/j.jallcom.2020.157386
0925-8388/

replace Ti^{4+} ions of $Li_2Mg_3TiO_6$ ceramics. Among them, $Li_2Mg_3Ti_{0.95}(Mg_{1/3}Sb_{2/3})_{0.05}O_6$ ceramics had great microwave dielectric properties ($\varepsilon_r = 14.6$, $Q \times f = 195{,}500$ GHz, $\tau_f = -4.02$ ppm/°C); $Li_2Mg_3Ti_{0.95}(Mg_{1/3}Nb_{2/3})_{0.05}O_6$ ceramics have also achieved great dielectric properties ($\varepsilon_r = 14.79$, $Q \times f = 204{,}900$ GHz, $\tau_f = -18.43$ ppm/°C). Zhang et al. [37] analyzed the correlation between the dielectric properties and sintering characteristics of $Li_{3+x}Mg_2Nb_{1-x}Ti_xO_6$ ($0.02 \le x \le 0.08$) ceramics. This improvement may be due to the different bonding between cations and oxygen ions in the oxygen octahedron. Therefore, it can be expected to improve the microwave dielectric performance by equivalent substitution at the cation position of the $Li_3Mg_2NbO_6$ ceramics.

In this work, we selected a set of data with the highest quality factor for analysis. We tested the dielectric properties of $Li_3Mg_2NbO_6$ ceramics when the doping amount of composite ions was 0.02–0.08. We found that when the doping amount was 0.04, the $Q \times f$ of the sample sintered at 1150 °C achieved the maximum value. The $Li_3Mg_2Nb_{0.96}(M_xW_{1-x})_{0.04}O_6$ ($M = Li^+$, Mg^{2+}, Al^{3+}, Ti^{4+}) ceramics were prepared by the solid-state reaction method. The dielectric properties, microstructure and structural characteristics of ceramics were systematically researched, such as $Li_3Mg_2Nb_{0.96}(Li_{1/5}W_{4/5})_{0.04}O_6$ (LMNLW), $Li_3Mg_2Nb_{0.96}(Mg_{1/4}W_{3/4})_{0.04}O_6$ (LMNMW), $Li_3Mg_2Nb_{0.96}(Al_{1/3}W_{2/3})_{0.04}O_6$ (LMNAW), and $Li_3Mg_2Nb_{0.96}(Ti_{1/2}W_{1/2})_{0.04}O_6$ (LMNTW).

2. Experimental section

High-purity oxide powders Nb_2O_5 (99.9%), WO_3 (99.9%), TiO_2 (99%), MgO (99.9%), Al_2O_3 (99%), Li_2CO_3 (97%) were used as raw materials according to $Li_3Mg_2Nb_{0.96}(M_xW_{1-x})_{0.04}O_6$ ($M = Li^+$, Mg^{2+}, Al^{3+}, Ti^{4+}) formula. Poured the raw material into nylon jars with ZrO_2 balls and add an appropriate amount of deionized water. Fixed the nylon jars on the planetary ball mill for 8 h. The mixtures were rapidly dried and calcined at 950 °C for 4 h to obtain the pre-sintering powders. Add 8 wt% paraffin as the binder in the sifted powder. The mixed paraffin powder was passed through an 80-mesh screen to form agglomerated spherical particles with good fluidity. The above mixture was pressed under the pressure of 2 ~ 3 MPa to produce a cylindrical of a certain thickness (10 mm × 5 mm). As shown in Fig. 1, to suppress the volatilization of lithium element, the cylinders were placed between two ceramic sheets (10 mm × 1.5 mm).

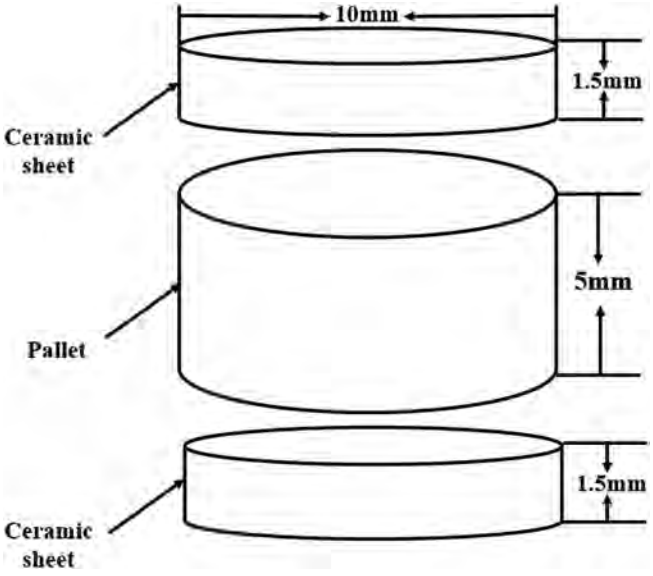

Fig. 1. Ceramic stacking method.

The X-ray diffraction (CuKα radiation, Rigaku D/max 2550 PC, 200kV/40 mA, Tokyo, Japan) was used to detect the crystalline phases of the $Li_3Mg_2Nb_{0.96}(M_xW_{1-x})_{0.04}O_6$ ($M = Li^+$, Mg^{2+}, Al^{3+}, Ti^{4+}) ceramics. Scanning electron microscope was used to characterize the microstructure of the samples (ZEISS MERLIN Compact, Germany). The dielectric constant and quality factor of samples were observed by a network analyzer (9–11 GHz, N5234A, Agilent Co., Santa Clara, CA). The temperature coefficient of resonant frequency (τ_f) was determined according to the following formula:

$$\tau_f = \frac{f_{85} - f_{25}}{f_{25}(T_{85} - T_{25})} \times 10^6 (ppm/^\circ C) \quad (1)$$

where f_{85} and f_{25} were the resonant frequencies at 85 °C and 25 °C, respectively.

The Archimedes method was used to measure the bulk density. The theoretical density was calculated by Eq. (2):

$$\rho_{th} = \frac{AZ}{N_A V} \quad (2)$$

where A was the atomic mass, Z was the number of molecules in a single unit cell, N_A was the Avogadro constant, and V was the unit cell volume.

The relative density was obtained as the following formula:

$$\rho_{re} = \frac{\rho}{\rho_{th}} \quad (3)$$

3. Results and discussion

Fig. 2 demonstrate the XRD patterns of the $Li_3Mg_2Nb_{0.96}(M_xW_{1-x})_{0.04}O_6$ ($M = Li^+$, Mg^{2+}, Al^{3+}, Ti^{4+}) ceramics sintering at 1150 °C. It is readily observed that all diffraction patterns can be indexed to a standard $Li_3Mg_2NbO_6$ phase (JCPDS #86–0346), no secondary phase is detected. As the illustration of Fig. 2, we can note that the peaks slightly displaced toward a higher 2θ angle with different substitution ions. The increase in the 2θ angle may be due to the radius of the substitution ions ($(Li_{1/5}W_{4/5})^{5+}$ (r = 0.632 Å, CN = 6), $(Mg_{1/4}W_{3/4})^{5+}$ (r = 0.63 Å, CN = 6), $(Al_{1/3}W_{2/3})^{5+}$ (r = 0.582 Å, CN = 6) and $(Ti_{1/2}W_{1/2})^{5+}$ (r = 0.6025 Å, CN = 6)) is smaller than the radius of the Nb^{5+} ion (r = 0.64 Å, CN = 6).

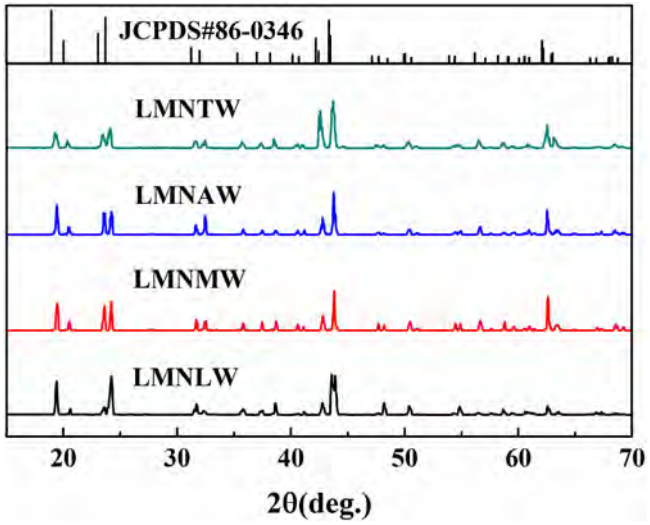

Fig. 2. The X-ray diffraction patterns of $Li_3Mg_2Nb_{0.96}(M_xW_{1-x})_{0.04}O_6$ (M = Li, Mg, Al, Ti) ceramics sintered at 1150 °C for 4 h.

To understand the relationship between the crystal structure and the complex ions ($(Li_{1/5}W_{4/5})^{5+}$, $(Mg_{1/4}W_{3/4})^{5+}$, $(Al_{1/3}W_{2/3})^{5+}$ and $(Ti_{1/2}W_{1/2})^{5+}$), the Rietveld method is used to refine the X-ray diffraction pattern. Based on the model of $Li_3Mg_2NbO_6$ ceramics, the Fullprof software is used to improve Rietveld. Fig. 3 shows the Rietveld refinement graph of the $Li_3Mg_2Nb_{0.96}$ $(M_xW_{1-x})_{0.04}O_6$ ($M = Li^+, Mg^{2+}, Al^{3+}, Ti^{4+}$) ceramics sintering at 1150 °C for 4 h. The lattice parameters (a, b and c), unit cell volumes (V), theoretical density (ρ_{theo}) and reliability factor (R_p, R_{wp}) of $Li_3Mg_2Nb_{0.96}$ $(M_xW_{1-x})_{0.04}O_6$ ($M = Li^+, Mg^{2+}, Al^{3+}, Ti^{4+}$) ceramics obtained by Rietveld refinement are displayed in Table 1. The values of reliability factor (patterns: R_p, weighted patterns: R_{wp}) are less than 15, manifesting that the results of refinement are superior.

Fig. 4 shows the microscopic morphology of $Li_3Mg_2Nb_{0.96}$ $(M_xW_{1-x})_{0.04}O_6$ ($M = Li^+, Mg^{2+}, Al^{3+}, Ti^{4+}$) ceramics sintered at 1150 °C. Fig. 4(a)–(d) show that the overall microstructures are dense and the grain boundaries are obvious, indicating that the grain growth of the obtained sample is well. The high $Q \times f$ values of the microwave dielectric ceramics may be related to the uniform grain morphology [38]. However, these external features are insufficient to explain the change in microwave dielectric properties of $Li_3Mg_2Nb_{0.96}$ $(M_xW_{1-x})_{0.04}O_6$ ($M = Li^+, Mg^{2+}, Al^{3+}, Ti^{4+}$) ceramics. Therefore, the relationship between microwave dielectric properties and intrinsic features must be researched.

Fig. 5 shows the ε_r and $Q \times f$ values of the $Li_3Mg_2Nb_{0.96}$ $(M_xW_{1-x})_{0.04}O_6$ ceramics sintered at different temperatures for 4 h. The ε_r and $Q \times f$ values of the $Li_3Mg_2Nb_{0.96}$ $(M_xW_{1-x})_{0.04}O_6$ ceramics reach a peak at 1150 °C and then decrease. Therefore, the optimal sintering condition is 1150 °C for all samples. As shown in Table 2, the relative densities of the samples sintered at 1150 °C exceeded 95% of the theoretical values. It may be possible to diminish the effect of density on the microwave dielectric properties of $Li_3Mg_2Nb_{0.96}$ $(M_xW_{1-x})_{0.04}O_6$ ceramics.

The dielectric constant is mainly related to density, secondary phase and ionic polarizability. From Fig. 2, there was no additional phase in all ranges. In addition, the relative densities of the samples are greater than 95%. In this paper, at the optimal sintering temperature, the dielectric constant of $Li_3Mg_2Nb_{0.96}$ $(M_xW_{1-x})_{0.04}O_6$ ceramics with different composite ions ($(Li_{1/5}W_{4/5})^{5+}$, $(Mg_{1/4}W_{3/4})^{5+}$, $(Al_{1/3}W_{2/3})^{5+}$ and $(Ti_{1/2}W_{1/2})^{5+}$) mainly depends on the ion polarizability. The observed dielectric polarizability (α_{obs}) was obtained according to the Clausius-Mosotti equation in Eq. (4) based on the observed dielectric constant:

$$\alpha_{obs} = \frac{3V_m(\varepsilon_r - 1)}{4\pi(\varepsilon_r + 2)} \tag{4}$$

where V_m and ε_r were the molar volume and the observed dielectric constant of samples, respectively. According to the addition rule of molecular polarizability, the theoretical ion polarizability (α_{theo}) of the samples could be decomposed into the molecular polarizability state of simple substances [39]:

$$\alpha_{theo} = 3\alpha_{Li^+} + 2\alpha_{Mg^{2+}} + 0.96\alpha_{Nb^{5+}} + 0.04x\alpha_M + 0.04(1-x)\alpha_{W^{5+}} + 6\alpha_{O^{2-}} \tag{5}$$

Table 1
The lattice parameters, unit cell volumes and theoretical densities of $Li_3Mg_2Nb_{0.96}$ $(M_xW_{1-x})_{0.04}O_6$ ceramics sintered at 1150 °C for 4 h.

Compositions	LMNLW	LMNMW	LMNAW	LMNTW
a(Å)	5.8912	5.8927	5.8903	5.8910
b(Å)	8.5594	8.5602	8.5562	8.5569
c(Å)	17.7140	17.7160	17.7085	17.7033
V(Å^3)	893.2309	893.6427	892.4833	892.4003
Rp	12.3	12.9	11.4	11.1
Rwp	13.7	13.8	12.8	11.6
ρ_{theo} (g/cm^3)	3.793	3.789	3.792	3.784

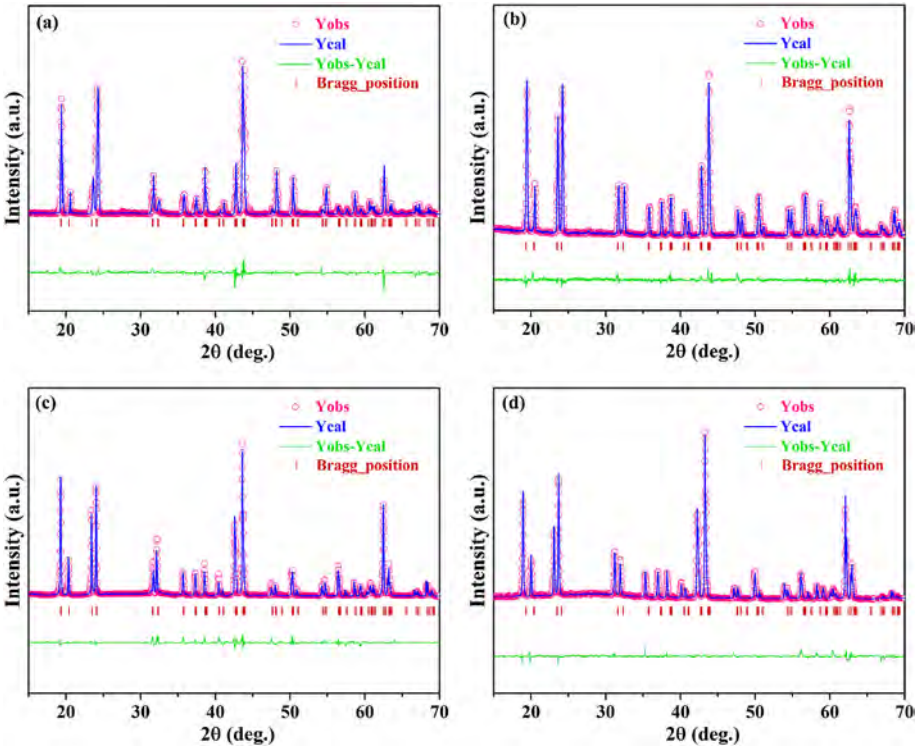

Fig. 3. Refinement patterns of $Li_3Mg_2Nb_{0.96}$ $(M_xW_{1-x})_{0.04}O_6$ (M = Li, Mg, Al, Ti) ceramics sintered at 1150 °C for 4 h.

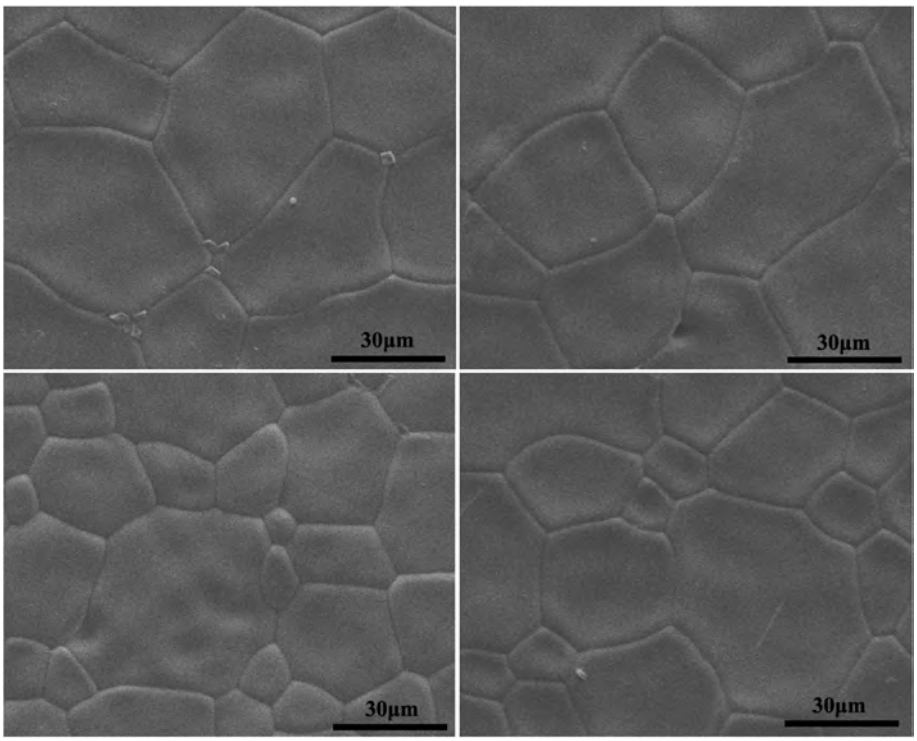

Fig. 4. The surface microstructures of $Li_3Mg_2Nb_{0.96}$ $(M_xW_{1-x})_{0.04}O_6$ ceramics sintered at 1150 °C for 4 h: (a) M = Li, (b) M = Mg, (c) M = Al, (d) M = Ti.

The results of ionic polarizability are listed in Table 2. The ε_{theo} of $Li_3Mg_2Nb_{0.96}$ $(M_xW_{1-x})_{0.04}O_6$ ceramics could be obtained by the Clausius-Mosotti equation [40]:

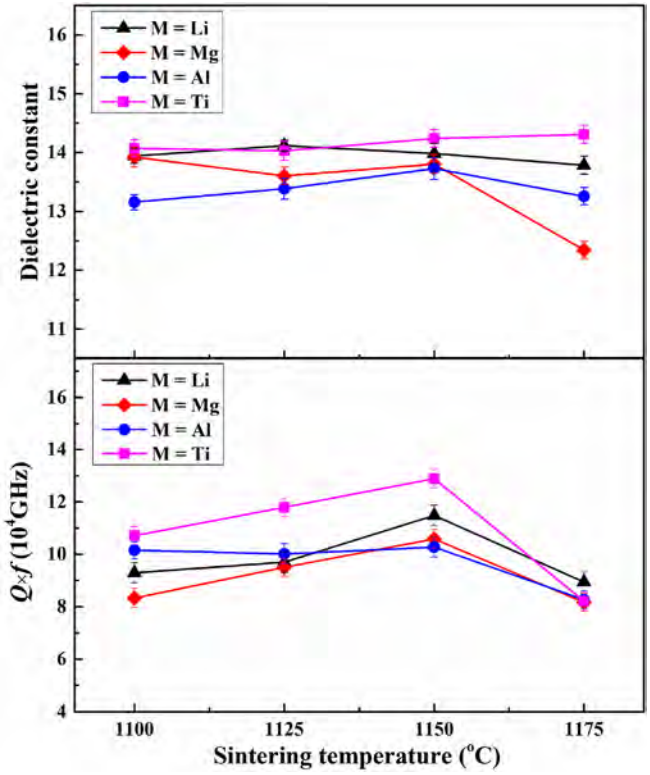

Fig. 5. The ε_r and $Q \times f$ values of the $Li_3Mg_2Nb_{0.96}$ $(M_xW_{1-x})_{0.04}O_6$ (M = Li, Mg, Al, Ti) ceramics sintered at different temperatures for 4 h.

$$\varepsilon_{theo} = \frac{3V_m + 8\pi\alpha_{theo}}{3V_m - 4\pi\alpha_{theo}} \quad (6)$$

Fig. 6 shows the change of observed dielectric constant (ε_r) of $Li_3Mg_2Nb_{0.96}(M_xW_{1-x})_{0.04}O_6$ ($M = Li^+, Mg^{2+}, Al^{3+}, Ti^{4+}$) ceramics as a function of theoretical dielectric constant (ε_{theo}). Although the ionic polarizabilities of $(Al^{3+}{}_{1/3}W^{6+}{}_{2/3})^{5+}$ (2.39 Å^3), $(Mg^{2+}{}_{1/4}W^{6+}{}_{3/4})^{5+}$ (2.73 Å^3), $(Li^{+}{}_{1/5}W^{6+}{}_{4/5})^{5+}$ (2.8 Å^3) and $(Ti^{4+}{}_{1/2}W^{6+}{}_{1/2})^{5+}$ (3.07 Å^3) are all different, neither the ionic polarizabilities (α_{obs}, α_{theo}) nor the dielectric constants (ε_r, ε_{theo}) change significantly with the type of substituted ion. As shown in Fig. 6 and Table 2, the ε_r, ε_{theo} and ion polarizabilities have the same trend. The results manifest the dielectric constant of $Li_3Mg_2Nb_{0.96}$ $(M_xW_{1-x})_{0.04}O_6$ ceramics is mainly affected by the ionic polarizability.

In this study, all samples are pure phase with orthogonal structure. The theoretical densities of the samples are close to the bulk densities. The $Q \times f$ values of dielectric materials are usually affected by density, grain size, miscellaneous phase, crystal structure and porosity [41,42]. Therefore, the influence of the second phase and density on the $Q \times f$ values of the samples can be ignored. The $Q \times f$ values of $Li_3Mg_2Nb_{0.96}$ $(M_xW_{1-x})_{0.04}O_6$ ceramics mainly depend on structural features, such as bond valence. To evaluate the structural characteristics, the bond valence (V_i) of $Li_3Mg_2Nb_{0.96}$ $(M_xW_{1-x})_{0.04}O_6$ ($M = Li^+, Mg^{2+}, Al^{3+}, Ti^{4+}$) ceramics could be calculated by the following formula [43,44]:

$$v_{i-o} = \exp\left[\frac{R_{i-o} - d_{i-o}}{b}\right] \quad (7)$$

$$V_i = \sum v_{i-o} \quad (8)$$

where the R_{i-o} was the bond valence parameter, d_{i-o} was the bond length between the atom i and o, and b was a universal constant (0.37 Å). The details of bond valence are given in Table 3. Fig. 7

Table 2
Physical properties of $Li_3Mg_2Nb_{0.96}(M_xW_{1-x})_{0.04}O_6$ ceramics sintered at 1150 °C for 4 h.

Compositions	Bulk Density (g/cm^3)	Relative Density (%)	V_m (Å^3)	α_{theo}	α_{obs}
LMNLW	3.6584	96.45	111.6538	22.2232	21.6049
LMNMW	3.6741	96.96	111.7053	22.2204	21.5521
LMNAW	3.6653	96.66	111.5604	22.2068	21.4937
LMNTW	3.6904	97.52	111.7926	22.2340	21.6514

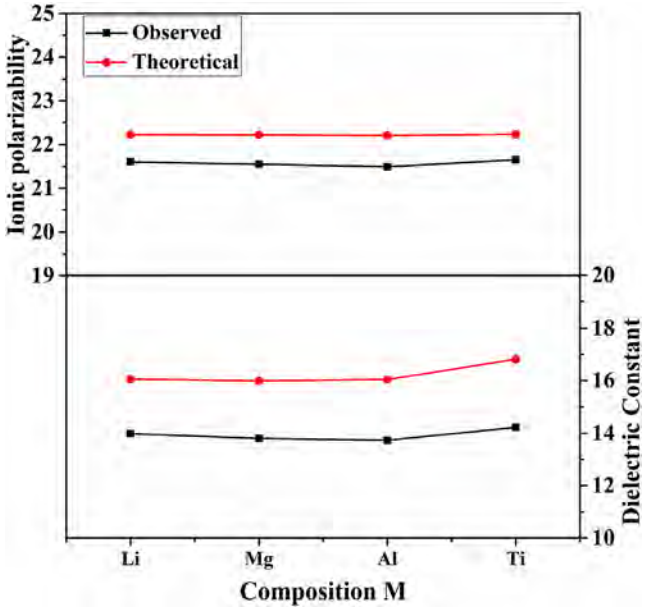

Fig. 6. (a) Theoretical polarizabilities (α_{theo}) and observed polarizabilities (α_{obs}), and (b) theoretical dielectric constants (ε_{theo}), and observed dielectric constants (ε_r) of the $Li_3Mg_2Nb_{0.96}(M_xW_{1-x})_{0.04}O_6$ (M = Li, Mg, Al, Ti) ceramics sintered at 1150 °C for 4 h.

shows the change of the $Q \times f$ values of $Li_3Mg_2Nb_{0.96}(M_xW_{1-x})_{0.04}O_6$ ceramics sintered at 1150 °C for 4 h as a function of average ionic bond valence. Previous studies [45,46] have shown that the bond valence was closely related to the strength of the chemical bond. High bond valence means that higher the strength of the chemical bond between cation and oxygen ions in the oxygen octahedron. High bond strength implies a lower lattice anharmonicity and damping constant of the microwave signal, resulting in a higher $Q \times f$ value. Therefore, the $Q \times f$ values of $Li_3Mg_2Nb_{0.96}(M_xW_{1-x})_{0.04}O_6$ ceramics depend on the bond valence. Compared with other samples, the LMNTW sample has the largest bond valence. LMNTW ceramics has the highest $Q \times f$ value (128,838 GHz). As shown in Table 4, the $Q \times f$ values of the samples in this work are much higher than the pure phase $Li_3Mg_2NbO_6$ ceramics [47]. Besides, $(M_xW_{1-x})^{5+}$ ions reduce the sintering

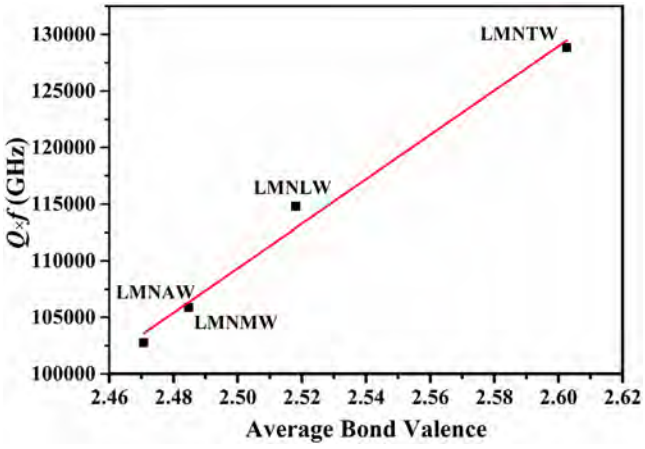

Fig. 7. Relationship between the $Q \times f$ values and the average bond valence of the $Li_3Mg_2Nb_{0.96}(M_xW_{1-x})_{0.04}O_6$ (M = Li, Mg, Al, Ti) ceramics sintered at 1150 °C for 4 h.

temperature of $Li_3Mg_2NbO_6$ ceramics ($Li_3Mg_2Nb_{0.96}(M_xW_{1-x})_{0.04}O_6$ ceramics ~ 1150 °C, $Li_3Mg_2NbO_6$ ceramics ~ 1250 °C).

Fig. 8 shows the relationship between the τ_f values and the average oxygen octahedral distortion of Li3Mg2Nb0.96(MxW1-x)0.04O6 ceramics sintered at 1150°C for 4h. Reaney et al. [48] reported that the τf values could be determined by the distortion of oxygen octahedron. The distortion of oxygen octahedrons was calculated by the following formula:

$$\Delta = \left(\frac{1}{6}\right) \times \sum \left[\frac{d_{i-o} - \bar{d}}{\bar{d}}\right] \quad (9)$$

where *di-o* was the bond length, and*d* was the average bond length between cations and anions in the oxygen octahedron. The changing trend of τ_f values is opposite to the average oxygen octahedral distortion, which is consistent with the conclusions reported previously. As shown in Fig. 8, the variation range of the τ_f values is very small, which shows that the replacement of W-based composite ions has little effect on the temperature coefficient of the resonance frequency of Li3Mg2NbO6 ceramics.

Table 3
Bond valence of $Li_3Mg_2Nb_{0.96}(M_xW_{1-x})_{0.04}O_6$ ceramics sintered at 1150 °C for 4 h.

Compositions	Bond valence							
	NbO_6	$(Li1\|Mg1)O_6$		$(Li2\|Mg2)O_6$		$(Li3\|Mg3)O_6$		Average
		$Li_{(1)}O_6$	$Mg_{(1)}O_6$	$Li_{(2)}O_6$	$Mg_{(2)}O_6$	$Li_{(3)}O_6$	$Mg_{(3)}O_6$	
LMNLW	5.2176	1.1922	2.0711	1.1908	2.0912	1.1235	2.0411	2.5181
LMNMW	5.0384	1.1954	2.0745	1.1962	2.0853	1.1542	2.0957	2.4847
LMNAW	4.9976	1.1893	2.0816	1.1896	2.0822	1.1387	2.0888	2.4707
LMNTW	5.5173	1.1854	2.0793	1.1859	2.0973	1.1379	2.1001	2.6026

Table 4
Dielectric properties of $Li_3Mg_2NbO_6$ ceramics with different doping ions.

Compositions	Sintering temperature (°C)	ϵ_r	$Q \times f$ (GHz)	τ_f (ppm/°C)
LMNLW	1150	13.9806	114781	−22.33
LMNMW	1150	13.8022	105879	−21.19
LMNAW	1150	13.7253	102760	−23.11
LMNTW	1150	14.2356	128838	−21.12
Pure LMN	1250	16.8	79643	−27.2

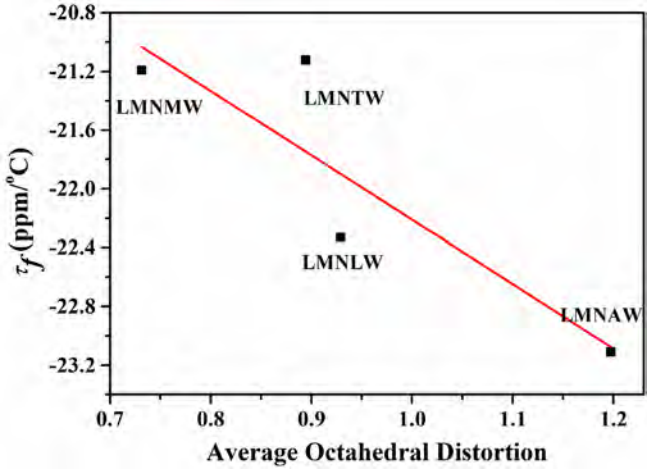

Fig. 8. Relationship between τ_f values and the average oxygen octahedral distortion of the $Li_3Mg_2Nb_{0.96}(M_xW_{1-x})_{0.04}O_6$ (M = Li, Mg, Al, Ti) ceramics sintered at 1150 °C for 4 h.

4. Conclusions

The novel $Li_3Mg_2Nb_{0.96}(M_xW_{1-x})_{0.04}O_6$ ($M = Li^+$, Mg^{2+}, Al^{3+}, Ti^{4+}) ceramics were prepared via the solid-state reaction method. XRD analysis results manifested that within the doping range, all samples were pure phase solid solutions. The microwave dielectric properties mainly depended on the lattice structure of the samples. The study found that the observed dielectric constant was completely consistent with the theoretical dielectric constant, indicating that the dielectric constant mainly depended on the ion polarizability. Based on the calculated results from the complex chemical bond theory, the variation trend of $Q \times f$ values were consistent with the average bond valence. The high $Q \times f$ value obtained by LMNTW was due to its higher average bond valence. The changing trend of τ_f values is opposite to the average oxygen octahedral distortion.

CRediT authorship contribution statement

Ping Zhang: Conceptualization, Methodology, Validation, Investigation, Data curation, Writing - original draft, Writing - review & editing, Resources. **Manman Hao:** Methodology, Validation, Writing - original draft, Data curation, Software. **Mi Xiao:** Methodology, Validation, Resources.

Declaration of competing interest

The authors declare that they have no known competing financial interests or personal relationships that could have appeared to influence the work reported in this paper.

Acknowledgments

This work was supported by Major Projects of Science and Technology in Tianjin (No. 18ZXJMTG00020) and the National Natural Science Foundation of China (No. 61671323).

References

[1] M. Makimoto, S. Yamashita, in: K. Itoh, T. Sakurai (Eds.), Microwave Resonators and Filters for Wireless Communication: Theory, Design and Application, Springer Science & Business Media, Springer-Verlag Berlin Heidelberg, New York, 2001, pp. 1–7.
[2] I.M. Reaney, D. Iddles, Microwave dielectric ceramics for resonators and filters in mobile phone networks, J. Am. Ceram. Soc. 89 (2006) 2063–2072.
[3] A.T. Vanderah, Talking ceramics, Science 298 (2002) 1182–1184.
[4] R. Peng, Y.X. Li, H. Su, Y.C. Lu, M.S. Chen, W. Du, B. Liao, Experiment and calculation: the Li(Zn, Mn)PO_4 solid solution ceramics with low dielectric constant, high quality factor, and low densification temperature, J. Alloys Compd. 842 (2020) 155709.
[5] R. Peng, Y.C. Lu, Z.H. Tao, D.M. Chen, L. Shi, Q. Zhang, Y.X. Lia, Improved microwave dielectric properties and sintering behavior of $LiZnPO_4$ ceramic by Ni^{2+}-ion doping based on frst-principle calculation and experiment, Ceram. Int. 46 (2020) 11021–11032.
[6] R. Peng, H. Su, D. An, Y.C. Lu, Z.H. Tao, D.M. Chen, L. Shi, Y.X. Lia, The sintering and dielectric properties modification of Li_2MgSiO_4 ceramic with Ni^{2+}-ion doping based on calculation and experiment, J. Mater. Res. Technol. 9 (2020) 1344–1356.
[7] S. Zhang, H. Su, H. Zhang, Y. Jing, X. Tang, Microwave dielectric properties of $CaWO_4$-Li_2TiO_3 ceramics added with LBSCA glass for LTCC applications, Ceram. Int. 42 (2016) 15242–15246.
[8] H. Shao, Z. Liu, G. Jian, Y. Li, Low-temperature sintering of $Ti_{1-x}Cu_{x/3}Nb_{2x/3}O_2$ (x = 0.23) microwave dielectric ceramics with CuO and B_2O_3 addition, Ceram. Int. 44 (2018) 3314–3318.
[9] Q. Guo, L. Li, S. Yu, Z. Sun, H. Zheng, J. Li, W. Luo, Temperature-stable dielectrics based on Cu-doped $Bi_2Mg_{2/3}Nb_{4/3}O_7$ pyrochlore ceramics for LTCC, Ceram. Int. 44 (2018) 333–338.
[10] H.H. Guo, D. Zhou, W.F. Liu, L.X. Pang, D.W. Wang, J.Z. Su, Z.M. Qi, Microwave dielectric properties of temperature-stable zircon-type (Bi, Ce)VO_4 solid solution ceramics, J. Am. Ceram. Soc. 103 (2020) 423–431.
[11] H.H. Guo, D. Zhou, L.X. Pang, Z.M. Qi, Microwave dielectric properties of low firing temperature stable scheelite structured (Ca,Bi)(Mo,V)O_4 solid solution ceramics for LTCC applications, J. Eur. Ceram. Soc. 39 (2019) 2365–2373.
[12] M. Castellanos, J.A. Gard, A.R. West, Crystal data for a new family of phases, $Li_3Mg_2XO_6$: X = Nb, Ta, Sb, J. Appl. Crystallogr. 15 (1982) 116–119.
[13] H.T. Wu, E.S. Kim, Correlations between crystal structure and dielectric properties of high-Q materials in rock-salt structure Li_2O-MgO-BO_2 (B = Ti, Sn, Zr) systems at microwave frequency, RSC Adv. 6 (2016) 47443–47453.
[14] J. Zhang, R.Z. Zuo, Synthesis and microwave dielectric properties of $Li_2Mg_2(WO_4)_3$ ceramics, Mater. Lett. 158 (2015) 92–94.
[15] D. Zhou, C.A. Randall, L.X. Pang, H. Wang, X.G. Wu, J. Guo, G.Q. Zhang, L. Shui, X. Yao, Microwave dielectric properties of $Li_2(M^{2+})_2Mo_3O_{12}$ and $Li_3(M^{3+})Mo_3O_{12}$ (M = Zn, Ca, Al, and in) lyonsite-related-type ceramics with ultra-low sintering temperatures, J. Am. Ceram. Soc. 94 (2011) 802–805.
[16] J. Zhang, R.Z. Zuo, Y. Wang, S.S. Qi, Phase evolution and microwave dielectric properties of $Li_4Ti_{5(1+x)}O_{12}$ ceramics, Mater. Lett. 164 (2016) 353–355.
[17] Y.G. Zhao, P. Zhang, Microstructure and microwave dielectric properties of low loss materials $Li_3(Mg_{0.95}A_{0.05})_2NbO_6$ (A = Ca^{2+}, Ni^{2+}, Zn^{2+}, Mn^{2+}) with rock-salt structure, J. Alloy, Compd 658 (2016) 744–748.
[18] P. Zhang, L. Liu, M. Xiao, Y.G. Zhao, A novel temperature stable and high Q microwave dielectric ceramic in $Li_3(Mg_{1-x}Mn_x)_2NbO_6$ system, J. Mater. Sci. Mater. Electron. 28 (2017) 12220–12225.
[19] P. Zhang, L. Liu, M. Xiao, Microwave dielectric properties of high Q and temperature stable $Li_3(Mg_{1-x}Ni_x)_2NbO_6$ ceramics, J. Mater. Sci. Mater. Electron. 29 (2018) 5057–5063.
[20] C.F. Xing, J.X. Bi, H.T. Wu, Effect of Co-substitution on microwave dielectric properties of $Li_3(Mg_{1-x}Co_x)_2NbO_6$ ($0.00 \le x \le 0.10$) ceramics, J. Alloys Compd. 719 (2017) 58–62.
[21] P. Zhang, X.S. Wu, M. Xiao, Effect of Sb^{5+} ion substitution for Nb^{5+} on crystal

structure and microwave dielectric properties for $Li_3Mg_2NbO_6$ ceramics, J. Alloys Compd. 766 (2018) 498–505.
[22] G. Wang, H.W. Zhang, X. Huang, F. Xu, G.W. Gan, Y. Yang, D.D. Wen, J. Li, C. Liu, L.C. Jin, Correlations between the structural characteristics and enhanced microwave dielectric properties of V-modified $Li_3Mg_2NbO_6$ ceramics, Ceram. Int. 44 (2018) 19295–19300.
[23] G. Wang, D.N. Zhang, X. Huang, Y. H Rao, Y. Yang, G.W. Gan, Y.M. Lai, F. Xu, J. Li, Y.L. Liao, C. Liu, L.C. Jin, V.G. Harris, H.W. Zhang, Crystal structure and enhanced microwave dielectric properties of Ta^{5+} substituted $Li_3Mg_2NbO_6$ ceramics, J. Am. Ceram. Soc. 103 (2019) 214–223.
[24] H.T. Wu, E.S. Kim, Characterization of low loss microwave dielectric materials $Li_3Mg_2NbO_6$ based on the chemical bond theory, J. Alloys Compd. 669 (2016) 134–140.
[25] G. Wang, D.N. Zhang, J. Li, G.W. Gan, Y. H Rao, X. Huang, Y. Yang, L. Shi, Y.L. Liao, C. Liu, L.C. Jin, H.W. Zhang, Crystal structure, bond energy, Raman spectra, and microwave dielectric properties of Ti-doped $Li_3Mg_2NbO_6$ ceramics, J. Am. Ceram. Soc. (2020) 1–12, 00.
[26] P. Zhang, K.X. Sun, M. Xiao, Crystal structure, densification, and microwave dielectric properties of $Li_3Mg_2(Nb_{(1-x)}Mo_x)O_{6+x/2}$ ($0 \leq x \leq 0.08$) ceramics, J. Am. Ceram. Soc. 95 (2018) 4127–4135.
[27] P. Zhang, M.M. Hao, X.R. Mao, K.X. Sun, M. Xiao, Effects of W^{6+} substitution on crystal structure and microwave dielectric properties of $Li_3Mg_2NbO_6$ ceramics, Ceram. Int. 46 (2020) 21336–21342.
[28] H.H. Guo, D. Zhou, C. Du, P.J. Wang, W.F. Liu, L.X. Pang, Q.P. Wang, J.Z. Su, C. Singhf, S. Trukhanov, Temperature stable $Li_2Ti_{0.75}(Mg_{1/3}Nb_{2/3})_{0.25}O_3$-based microwave dielectric ceramics with low sintering temperature and ultra-low dielectric loss for dielectric resonator antenna applications, J. Mater. Chem. C. 8 (2020) 4690–4700.
[29] P. Zhang, H. Xie, Y.G. Zhao, M. Xiao, Low temperature sintering and microwave dielectric properties of $Li_3Mg_2NbO_6$ ceramics doped with Li_2O-B_2O_3-SiO_2 glass, J. Alloys Compd. 690 (2017) 688–691.
[30] P. Zhang, L. Liu, Y.G. Zhao, M. Xiao, Low temperature sintering and microwave dielectric properties of $Li_3Mg_2NbO_6$ ceramics for LTCC application, J. Mater. Sci. Mater. Electron. 28 (2017) 5802–5806.
[31] P. Zhang, X.Y. Zhao, Y.G. Zhao, Effects of MBS addition on the low temperature sintering and microwave dielectric properties of $Li_3Mg_2NbO_6$ ceramics, J. Mater. Sci. Mater. Electron. 27 (2016) 6395–6398.
[32] P. Zhang, J.W. Liao, Y.G. Zhao, X.Y. Zhao, M. Xiao, Effects of B_2O_3 addition on the sintering behavior and microwave dielectric properties of $Li_3Mg_2NbO_6$ ceramics, J. Mater. Sci. Mater. Electron. 28 (2017) 686–690.
[33] E.S. Kim, S.N. Seo, Dependence of dielectric properties on structural characteristics of $(Zn_{1/3}A_{2/3})_{0.5}(Ti_{1-x}B_x)_{0.5}O_2$ (A = Nb^{5+}, Ta^{5+}, B = Ge^{4+}, Sn^{4+}) ceramics at microwave frequencies, J. Eur. Ceram. Soc. 30 (2010) 319–323.
[34] H.J. Jo, E.S. Kim, Enhanced quality factor of $MgTiO_3$ ceramics by isovalent Ti-site substitution, Ceram. Int. 42 (2016) 5479–5486.
[35] H.L. Pan, Y.W. Zhang, H.T. Wu, Crystal structure, infrared spectroscopy and microwave dielectric properties of utra low-loss $Li_2Mg_3Ti_{0.95}(Mg_{1/3}Sb_{2/3})_{0.05}O_6$ ceramic, Ceram. Int. 44 (2018) 3464–3468.
[36] Y. K Yang, H.L. Pan, H.T. Wu, Crystal structure, Raman spectra and microwave dielectric properties of $Li_2Mg_3Ti_{0.95}(Mg_{1/3}Nb_{2/3})_{0.05}O_6$ ceramic, Ceram. Int. 44 (2018) 11350–11356.
[37] P. Zhang, K.X. Sun, X.R. Mao, M. Xiao, Z.T. Zheng, Crystal structures and high microwave dielectric properties in Li^+/Ti^{4+} ions co-doped $Li_3Mg_2NbO_6$ ceramics, Ceram. Int. 46 (2020) 8097–8103.
[38] Z. Gong, Z. Wang, L. Wang, Z. Fu, W. Han, Q. Zhang, Microwave dielectric properties of high-Q $Mg(Sn_xTi_{1-x})O_3$ ceramics, Electron. Mater. Lett. 9 (2013) 331–335.
[39] R.D. Shannon, G.R. Rossman, Dielectric constants of silicate garnets and the oxide additivity rule, Am. Mineral. 77 (1992) 94–100.
[40] R.D. Shannon, Dielectric polarizabilities of ions in oxides and fluorides, J. Appl. Phys. 73 (1993) 348–366.
[41] Y. Zhang, Y.C. Zhang, M.Q. Xiang, Crystal structure and microwave dielectric characteristics of Zr-substituted $CoTiNb_2O_8$ ceramics, J. Eur. Ceram. Soc. 36 (2016) 1945–1951.
[42] J. Song, J. Zhang, R. Zuo, Ultrahigh Q values and atmosphere-controlled sintering of $Li_{2(1+x)}Mg_3ZrO_6$ microwave dielectric ceramics, Ceram. Int. 43 (2017) 2246–2251.
[43] I.D. Brown, D. Altermatt, Bond-valence parameters obtained from a systematic analysis of the inorganic crystal structure database, Acta Crystallogr. 41 (1985) 244–247.
[44] I.D. Brown, K.U. Kang, Empirical parameters for calculating cation-oxygen bond valences, Acta Crystallogr. 32 (1976) 1957–1959.
[45] J. Li, Y. Han, T. Qiu, C. Jin, Effect of bond valence on microwave dielectric properties of (1-x)$CaTiO_{3-x}(Li_{0.5}La_{0.5})TiO_3$ ceramics, Mater. Res. Bull. 47 (2012) 2375–2379.
[46] S.K. Singh, V.R.K. Murthy, Crystal structure, Raman spectroscopy and microwave dielectric properties of layered-perovskite $BaA_2Ti_3O_{10}$ (A = La, Nd and Sm) compounds, Mater. Chem. Phys. 160 (2015) 187–193.
[47] L.L. Yuan, J.J. Bian, Microwave dielectric properties of the lithium containing compounds with rock salt structure, Ferroelectrics 387 (2009) 12–123.
[48] I.M. Reaney, E.L. Colla, N. Setter, Dielectric and structural characteristics of Ba-and Sr-based complex perovskites as a function of tolerance factor, Jpn. Appl. Phys. 33 (1994) 3984–3990.